

A Simulation Study of Alternans-Arrhythmia Based on Physiology of Invertebrate Heart

Toru Yazawa, Hiroyuki Kitajima, and Akira Shimizu

Abstract—Alternans is an arrhythmia exhibiting alternating amplitude/interval from beat to beat on heartbeat recordings, such as the finger pulse. Alternans is well known since Traube's document in 1872 and is called harbinger of death, but the mechanisms for its generation is not fully defined and much work still remains. We studied this abnormal state of the heart, in animal models (electrophysiology) and with a numerical model (computer simulation). We focused our attention on a causal association between the pace-making cells and ventricular cells. We revealed that one of the main causalities in generating alternates was a potassium ionic abnormality. We discussed the concentration of ions in the extracellular space of the heart-tissue.

Index Terms—alternans, EKG, lobster hearts, potassium, simulation

I. INTRODUCTION

A persimmon tree in my (TY) garden bears rich fruits every other year. Atmospheric oxygen on the earth has bistability [1, 2]. Period-2 is an intriguing rhythm in nature's environment. The cardiac alternans is another intriguing period-2 phenomena. Since the cardiac period-2 was described by Traube (1872), alternans has remained an electrocardiographic curiosity for more than three quarters of a century [3, 4].

In our physiological experiments on the crustaceans in the 1980's, we have noticed that alternans was frequently observable with the "isolated" hearts (Note: The heart sooner or later dies in the experimental dish). We realized that it was a sign of future cardiac cessation. Nowadays, researchers believe that alternans is the harbinger for sudden death [3, 5]. So, we came back to the crustacean physiology. Details of alternans have not been studied in crustaceans. But, we considered that model studies may contribute to the advance in management of the dysfunction of a complex cardiovascular disease.

In the worst case scenario alternans triggers a cardiac

Manuscript received July 2, 2013; revised July 18, 2013. This work was supported in part by a Grant-in-Aid for Scientific Research No. 23500524 (TY) and No. 23500367 (HK). We thank DVX Inc. Tokyo, Japan, for financial support, research No. 4DQ404.

T. Yazawa is with the Neurobiology Laboratory, Tokyo Metropolitan University, Hachioji, 192-0397 Tokyo, Japan (phone: +81-426771111; email: yazawa-tohru@tmu.ac.jp).

H. Kitajima is with the Electric Engineering Department, Kagawa University, Hayashi, Takamatsu, 761-0396 Japan (e-mail: kitaji@eng.kagawa-u.ac.jp).

A. Shimizu is with the Systematic Zoology Laboratory, Tokyo Metropolitan University, Hachioji, 192-0397 Tokyo, Japan (e-mail: shimizu-akira@tmu.ac.jp).

instability (e.g. ventricular arrhythmias) and causes a sudden cardiac death [6]. Reducing the risk of sudden death is a goal of research in physiology and technology, but mechanisms for the generation of alternans have not been fully understood. The cardiovascular system (CVS) of us humans and those of invertebrates resemble each other because of evolution, and the invertebrate cardiac physiology has an over 100 years of history. Those animal's CVS has been evolved since millions of years, before our human system developed. Our human system is fundamentally a copy of them. We thus tried to study alternans, using experimental data on animal models, with a newly assembled mathematical model (Kitajima and Yazawa 2010). A computer simulation regarding to alternans rhythm based on the real-world crustacean data has not been conducted before.

II. MATERIALS AND METHODS

A. Heartbeat Recording

Ethics

All subjects were treated as per the ethical control regulations of the Tokyo Metropolitan University.

Human Heartbeat

We used the finger pulse recordings with a piezoelectric sensor, connected to a Power Lab System (PLab, AD Instruments, Australia).

Animal Heartbeat

The electrocardiogram (EKG) from model animals were recorded by implanted metal electrodes, connecting to an amplifier (usually 10,000 magnification, DAM50, WPA, USA) and then to the PLab. The PLab digitized data at 1 kHz.

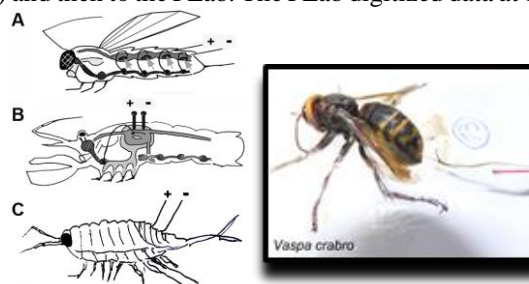


Fig. 1. EKG methods. A, insect; B, lobster/crayfish; C, *Ligia*.

Intact Hearts (Animal Model)

To analyze intact heartbeats, stored EKGs (FM-tape and/or PC) and newly recorded EKGs were used. Animal EKGs were obtained from following animals (Fig. 1): The hornet, *Vespa* sp. (n = 17, Fig. 1A, see inset picture), the

lobsters, *Homarus americanus* (n = more than 50, Fig. 1B), the crayfish, *Procambarus clarkii* (n = more than 100), and the sea lice, *Ligia exotica* (n = 3, Fig. 1C).

Isolated Heart (Animal Model)

We prepared an isolated heart (Fig. 2 for experimental set-up) to record membrane potential (P) and contraction force (F) of the heart. A hanging glass capillary micro-electrode was used to monitor intracellular membrane potential of moving heart (Fig. 2).

To record pace-maker activities, we opened the heart from ventral side. The pace-maker cells (CG in Fig. 2) are located on the dorsal lumen of the ventricle. The pace-maker activities (CG in Fig. 2) were recorded by extracellular recording methods. Contraction of the heart was also recorded mechanically by a force transducer (F in Fig. 2). We used isolated *ostium muscle* (OOM) to investigate E-C coupling of the heart muscle [7, 8] (see below).

B. Animal Heart Evolution

The human heart develops from beating tubes. Folding-tube is a key process to make a four chambered heart (Fig. 3, C1, C2, and C3). A vertebrate gene, *Nkx2-5*, works for the heart development (Fig. 3). A fly gene, *tinman*, which is an orthologue gene of *Nkx2-5*, works for a fly tube heart (Fig. 3A). In turn, the lobster has a single chamber heart (Fig. 3D). Evolutional link between the tube-heart and the chamber-heart is explained in Fig. 3B: A hypothetical evolution, linking *Squilla* heart to *Homarus* heart [9]. The existence of this hereditary trait suggest that crustacean hearts and human hearts are fundamentally the same, in terms of morphology and physiology.

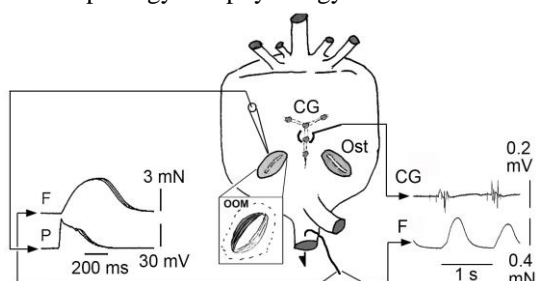


Fig. 2. Isolated heart experiments. Recordings of muscle action potential (P), force of contraction (F), and extracellular recording of the cardiac ganglionic pacemaker impulses (CG). *Homarus* heart, ventral view. The CG is attached to the dorsal lumen of the heart, therefore the CG can be seen, if the heart is opened. Inset, an isolated ostium, OOM (*musculus orbicularis ostii*) (see [7, 8]).

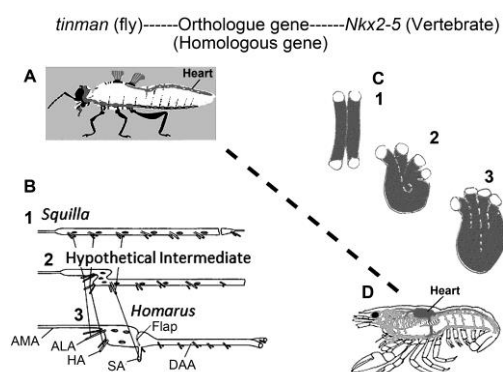


Fig. 3. Evolution of the heart: Link between arthropods and vertebrates. AMA; anterior median artery; ALA, anterior lateral artery; HA, hepatic artery; SA, sternal artery; DAA, dorsal abdominal artery.

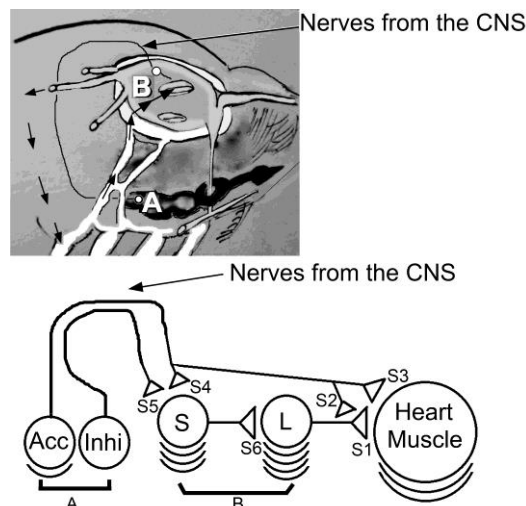


Fig. 4. Crustacean cardio-regulatory system. Arrows indicate the direction of blood flow: Leaving from the heart, passing through arteries, body cavity, gills near legs, pericardial sinus, and ostia to return to the heart. The central nervous system (CNS) (A) sends autonomic nerve fibers to the pace-maker (B) and the heart muscle [12]. Postulated neurotransmitters working at synapses are: S1, S2, S3, S4: glutamate [10, 11, 12]. S5: GABA [12]. S6: acetylcholine [13].

C. Heartbeat Regulation

To adjust to peripheral demands and to propel blood efficiently, the heart needs to receive controls. The cardiac control center is located in the sub-esophageal ganglion (A in Fig. 4). This center is homologous to the human autonomic center for the heart. In crustaceans, the center (A) sends two types of nerves to the heart: acceleratory and inhibitory axons (see the nerve-circuit diagram in Fig. 4). The cardio-regulatory nerves innervate both the pace-maker (B) and the heart muscle. B is composed of small-sized pace-maker cells (S) and large-sized pace-maker cells (L) (Fig. 4). The muscle cells receive periodic stimuli from L (Fig. 4). B is called as the cardiac ganglion (CG) (see CG in Fig. 2A), and B also works as a switch board or a relay circuit, transferring central commands to heart muscle. Heart muscles send feedback information to the CG [15]. Interestingly, in human, the heart has “the cardiac ganglions/plexus” too. The structure and function of the heart-control network of invertebrates are similar to that of vertebrates. Fundamental architecture is hereditary in evolution: a pump and a controller.

Six types of identified synapses (S1 to S6) are documented in the network (Fig. 4). In the present paper, we focus on the synapse S1 among them. The chemical synapse S1 connects L-cells to muscle. We investigated this connection, focusing attention on the mechanisms of alternans arising at the L-S1-Muscle system.

III. RESULTS

Alternans is observable in human patients with heart failure. Alternans is thought as the harbinger of sudden death because alternans is known to advance to atrial fibrillation. Alternans might thus be a terminal sign, but much work remains to do. When and what conditions does the heart exhibit alternans?

A. Empirical Alternans

Animal Model

We succeeded to record alternans EKGs (insects and crustaceans, see Fig. 1). Generally, alternans occurred hours before specimens passed away.

In insects (we tested 16 hornets *Vespa mandarinia* and *Vaspa crabro*, 13 bumblebees, *Bombus ardens*, five large carpenter bees, *Xylocopa appendiculata*, and two dragonflies, *Anotogaster sieboldii* and so forth), alternans phenomena were observable (example Fig. 5) if EKG electrodes were inserted properly (quick enough, i.e., almost no bleeding) (see Fig. 1 for recording methods, specimens immobilized).

In crustaceans (*Ligia exotica*, see Fig. 1C), alternans was also observable (Fig. 5): alternans appeared before heart rate dramatically increased. Then, specimens died after EKG gradually became small in amplitude. We observed such alternans phenomena in many crayfishes, many lobsters (*Pnulus japonicus*, *Homarus americanus*), and crabs (the coconut crab *Birgus latro* n = 4, the mokuzu crab *Eriocheir japonicus* n = 3, and the saw tooth gazami crab *Scylla serrata* n = 2).

Human Subjects

Human period-2 heartbeats were observable (Fig. 6). Fig. 6 shows period-doubling bifurcations, We can see not only two beats (Fig. 6C dashed line) but also four beats (see dots in Figs. 6B and 6C). We so far did not meet eight beats pumping.

Contraction and Potassium

Fig. 5 shows that amplitude of EKG swing decreased over time. This decrease in amplitude reflects gradual depolarization of muscle cells over time: The more membrane depolarize, the more amplitude decrease, and the more heart rate increase. Human terminal patients such as a cancer patient show the same phenomena, i.e., an increased heart rate, where the patients exhibits edema-swelling symptom. The edema-swelling is caused by necrosis of cells in various organs: intracellular potassium leaking from the cells to extracellular space. This can happen at the terminal condition. In Fig. 6, heart rate is not increased (heart rate, 60-80). She is alive over five years since this recording was taken.

In conclusion, these intact heart results suggest that necrosis-induced depolarization at the terminal condition caused alternans. We thus confirmed that alternans is a terminal sign as previously pointed out.

Arousal Alternans

Fig. 7 shows that heart rate dramatically increased and alternans appeared during a high rate beating, when a "sleeping" crayfish "woke up" to an "arousal state" (arrows \longleftrightarrow indicate alternans). We converted Fig. 7A data to Fig. 7B with "100 millisecond delay-time embedment" (see Tarkens [14]). This map clearly shows two distinctive alternate pulses. One can see that tails of orbit of large contractions are unstable (Fig. 7B arrowhead). This indicates that termination of muscular action potential by potassium

current (Hodgkin and Huxley theorem) was unstable. Instability of reversal potential of potassium ions is perhaps involved. We observed over 50 alternans from this crayfish, within a continuous 37 hr EKG recording. Alternans appeared at maximum speed of beating, induced by the cardio-acceleratory nerves. This alternans is not a terminal sign, because amplitude of EKG is large in swing size (i.e., hyperpolarization instead of depolarization, see Fig. 5). We interpreted that the cardiac nerves contributed to the induction of this alternans, also a possibility of hormone contribution. Signal molecules are at least key inducers of alternans. Alternans is apparently complex phenomena. In conclusion, membrane depolarization, membrane excitation (spike-generation), calcium (Ca^{2+}) handling (extracellular Ca^{2+} , intracellular Ca^{2+} , ryanodine receptor efficiency, and endoplasmic-reticulum (ER) Ca^{2+} amount) all of them are interconnected to generate alternans. A control mechanism behind alternans works to link nonlinearly all elements.

Isolated Muscle Alternans

We isolated OOM (see Fig. 2) and stimulated OOM every 1 to 2 sec (field stimulation with platinum (Pt) electrodes) and measured membrane potential (E) and force (F) of contraction (Fig. 8, inset). Bath application of a crustacean cardio-active neurohormone (proctolin, 10^{-9} mol/L, perfused for 2 min from an arrowhead) induced depolarization, and augmentation of stimulus-induced contractions (Fig. 8A). To our surprise, the stimulus induced spontaneous membrane oscillation and cyclic contraction (Fig. 8B). Period doubling (BPM trace) but less noticeable amplitude alternans (mV trace) can be seen in this case. Signal molecules, such as FMRF-amid like crustacean cardio-active peptide hormones, often induced similar oscillation and alternans (data not shown). This isolated muscle experiments indicated that muscle itself has ability to generate spontaneous alternans without regular cyclic timing signals.

Remarks for Empirical Results

Physiological tests are not enough for understanding complex causal connection behind alternans induction. We tried simulation study based on model animals' physiology data.

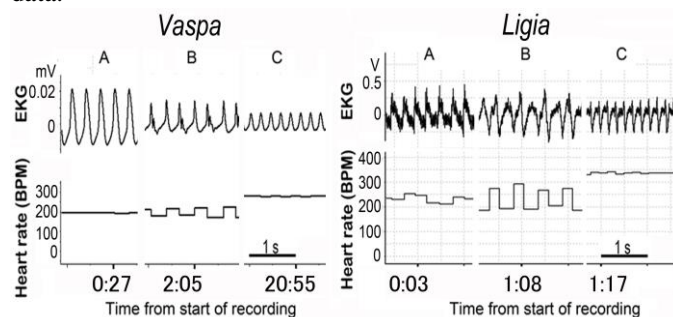


Fig. 5. EKGs of the hornet, *Vespa* sp. and the sea lice, *Ligia exotica*. Vespa: A, normal regular beating 27 min after start of recording (insect's anti-peristaltic beating, not referred to in this article). B, period-2, two hours after start of recording. C, heart rate dramatically increased, 20 hours. The heartbeat disappeared one min. after this recording. Ligia: A, regular heartbeat, three min. after start of recording. B, period-2, one hour. C, heart rate dramatically increased. The heartbeat disappeared two min after this recording.

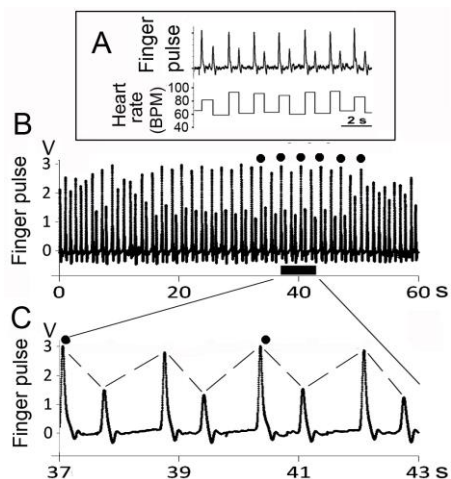


Fig. 6. Human alternans. A patient who suffered a cancer, diabetes, and kidney problems. Female age 60s. A wife of an author's (TY) friend kindly and willingly gave us her pulses.

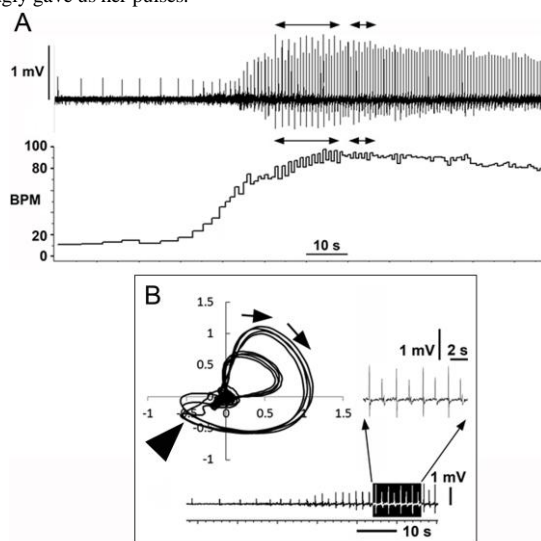


Fig.7 Crayfish alternans. A, during arousal behavior. B, Phase-space representation of Fig. 8A. One-second delay time embedment [see 14].

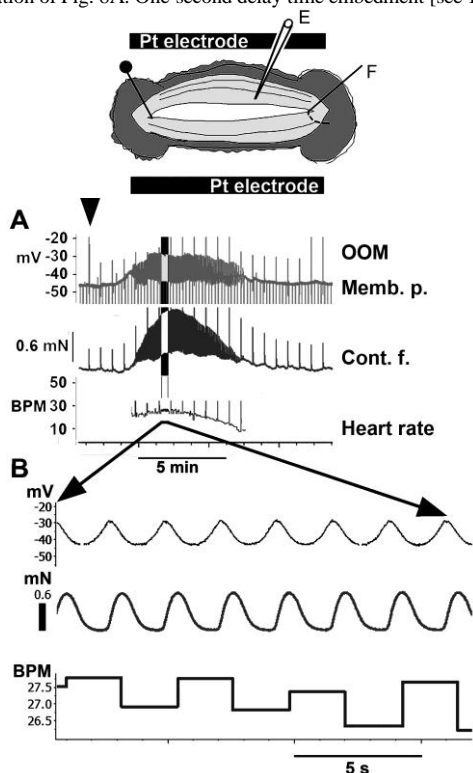


Fig. 8 Lobster OOM isolated muscle experiments.

B. Alternans Simulation

Mathematical Models

Studies of alternans using mathematical models are important for reducing the risk of sudden death. Previous modeling studies used difference equations for modeling alternans: revealing that generation of alternans is related to the period-doubling bifurcation or the border-collision bifurcation [16]. More realistic models using partial differential equations are proposed: revealing the dependency of $[K]_o$ (extracellular concentrations of potassium ions) [17] and influence of ionic conductance on alternans [18].

Human ventricular muscle cells receive electric stimulus from the pacemaker cells. Shape of the signals is characterized by a unique potential shape, that is, the diastolic slow depolarization (for an example, see Fig. 8B, mV-trace). However, in the previous modeling studies, the shape of stimulus was a rectangular wave. The coupling scheme from the pacemaker cells to the ventricular cells was not incorporated into these modeling. In contrast, we (Fig. 9A) used real synaptic potential shape [7] for modeling [19].

The network structure of the heart and nerves is known (see Fig 4). The identified synapse is S1 (see Fig. 4, from L to muscle), which is the target synapse in the present paper. We considered S1 is a key element in the L-S1-muscle architecture [7].

In the present paper, we used a simpler model, which has been previously published as the congress papers [19, 20]. The previous publications were lacking detailed consideration about the rationality between empirical real-world data and numerical simulation data. We demonstrate here the evaluation of our challenge of simulation by presenting real-world data as abovementioned.

By numerical analysis of our model we obtained results that two parameters (the conductance of the sodium ion and concentration of the potassium ion in the extracellular space) play key roles of generating alternans (see below).

LR Model with Synaptic Current

In Fig. 4 diagram, we only considered the sub-network of the pacemaker to the muscle cell (i.e., L-S1-muscle), as the first step of our study. For L and muscle we used the YNI model (Yanagihara-Noma-Irisawa) [21] and LR I model (Luo-Rudy I) [22] model, respectively. We treated L as the pacemaker cell. Considering the synaptic current from the pacemaker cell to the muscle cell, the dynamics of the pacemaker cell do not affect that of the muscle cell. Thus in this study we only consider the muscle cell with a periodic force. The period of the external force (usually called BCL: basic cycle length) is assumed to be 380 [msec]. The membrane potential V of the LR model with the synaptic input is described by

$$C \frac{dV}{dt} = -(I_{Na} + I_{Ca} + I_K + I_{K1} + I_{Kp} + I_b + I_{syn}) \quad (1)$$

where the meaning and the equations for each current is given in Appendix. The synaptic current I_{syn} from L to the muscle cells is given by

$$I_{syn} = G_{syn} (V - V_{syn}) s(t^*) \quad (2)$$

where G_{syn} is the maximum synaptic conductance, V_{syn} is the reversal potential and $s(t^*)$ is given by

$$s(t^*) = \frac{\tau_1}{\tau_2 - \tau_1} \left(-\exp\left(-\frac{t^*}{\tau_1}\right) + \exp\left(-\frac{t^*}{\tau_2}\right) \right) \quad (3)$$

where τ_1 and τ_2 are the raise and the decay time of the synapse, respectively. We identified these value 18 ms and 288 ms, respectively, from the experimental data (see Fig. 9A). We adjusted this crustacean values to mouse model. In mouse model, BCL is 1200 ms. Crustacean BCL was 380 ms in the present model. Thus, our two values for τ_1 and τ_2 are now 5.5 and 90, respectively (see Fig. 9A). t^* is the time which is reset at every nT (n is an integer and T is BCL).

Approximation of Discontinuous Functions

In Eq. (1), I_{Na} and I_K are given by

$$I_{Na} = G_{Na} m^3 h j (V - E_{Na}), \quad I_K = G_K X X_i (V - E_K)$$

where E_{Na} and E_K are the reversal potential, G_{Na} and G_K are the maximum ionic conductance for sodium (Na+) and potassium (K+) current, respectively, and m , h , j , and X are given by

$$\frac{dy}{dt} = \frac{y_{\infty} - y}{\tau_y}, \quad (y = m, h, j, X) \quad (4)$$

$$\tau_y = \frac{\tau_y}{\alpha_y + \beta_y}, \quad y_{\infty} = \frac{\alpha_y}{\alpha_y + \beta_y}. \quad (5)$$

Here, α_j , β_j , α_h , β_h , and X_i are described by discontinuous functions. For example, β_j and X_i are given by for $V \geq -40$

$$\beta_j(V) = \frac{0.3 \cdot \exp(2.535 \cdot 10^{-7} V)}{1 + \exp[-0.1(V+32)]} \quad (6)$$

for $V < -40$

$$\beta_j(V) = \frac{0.1212 \cdot \exp(-0.01052V)}{1 + \exp[-0.1378(V+40.14)]} \quad (7)$$

for $V > -100$

$$X_i(V) = \frac{2.837 \cdot (\exp[0.04(V+77)] - 1)}{(V+77) \cdot \exp[0.04(V+35)]} \quad (8)$$

for $V \leq -100$

$$X_i(V) = 1.0. \quad (9)$$

Considering a large number of neurons, discontinuous functions switched by some threshold values are not suitable for bifurcation analysis, because the algorithm becomes complicated. We adopted the continuous functions version of the Luo-Rudy model using sigmoidal functions. For example, $\beta_j(V)$ in Eq. (6) and (7) were combined into one equation

$$\beta_j(V) = \text{Eq. (6)} \cdot 0.5(1 + \tanh\{100 * (V + 40)\}) + \text{Eq. (7)} \cdot 0.5(1 + \tanh\{-100 * (V + 40)\}). \quad (10)$$

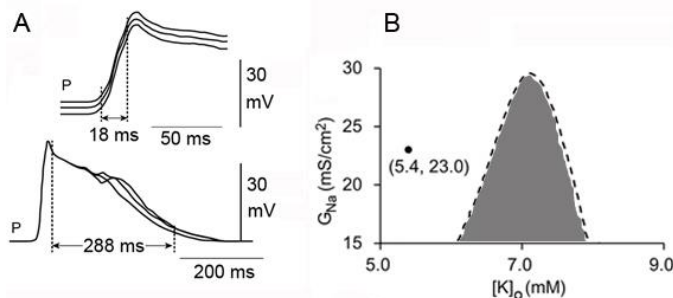


Fig. 9. A, configuration of the synaptic potential (recording methods, see Fig. 2). B, simulation, $[K]_o$ vs. G_{Na} .

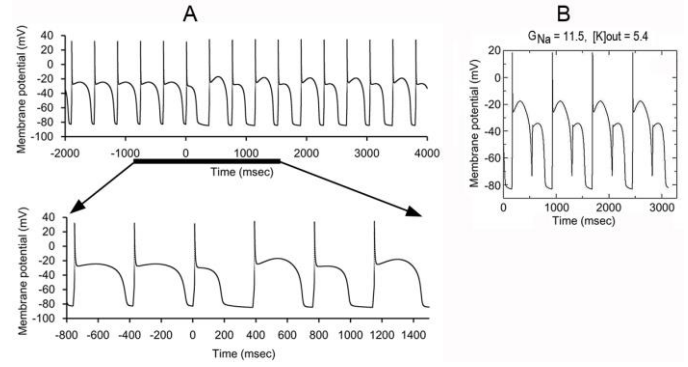


Fig. 10. Alternans simulation. A, period-doubling bifurcation. At time zero, $[K]_o$ was switched from 5.4 (normal) to 7.0 (edema). B, The saddle-node bifurcation but not alternans.

Simulation Results

We have already shown the effectiveness of the approximation (Eq. (10)) [20]. The approximation worked well and we observed periodic solutions [20]. We studied bifurcation phenomena correlated to alternans in the model. The value of the parameter related with are fixed as $G_{syn} = 4.0$, $V_{syn} = -29$.

Fig. 9B shows a two-parameter bifurcation diagram on the parameter plane $[K]_o$ (extracellular concentrations of potassium ions) and G_{Na} (the conductance for the sodium current). In this parameter region we observed two types of periodic two-periodic solutions, the period-doubling bifurcation and the saddle-node bifurcation [20]. The period-doubling bifurcation was alternans (Fig. 9B in gray region, Fig. 10A). Simulation spikes (Fig. 10A) apparently resembles with physiological spikes. The saddle-node bifurcation was not alternans (at G_{Na} below 12 mS/cm², scale out in Fig. 9B, see Fig. 10B an example trace).

Fig. 9B shows the area of the period-doubling. The closed circle (5.4, 23.0) indicates normal blood condition, i.e., the original values of the parameters. This simulation results indicate that alternans can be generated within a certain range of extracellular potassium concentration, from 6 to 8 if G_{Na} is fixed to 15. With a normal G_{Na} (23.0), alternans can be induced only at $[K]_o$ around 7 mM.

If $[K]_o$ increased from normal value 5.4 to up high, according to the Nernst equation (see Appendix, E_{Kl}), we can predict that the equilibrium potential shift toward depolarizing direction. The more K+ leaks, the more membrane depolarizes.

Empirical data (Fig. 2) suggested that excessively developed necrosis symptom does not exhibit alternans. (see Fig. 2, *Vaspa C* and *Liga C*). The simulation supported our physiological explanation why alternans disappear at a terminal state. We can explain it is due to a high value of potassium in tissue fluid. Simulation result was understandable and thus successful in the present analysis.

IV. DISCUSSION

In this paper we investigated the mechanism of generating alternans in the single model with the synaptic current. In most of previous studies the control parameter for generating alternans was period of an external stimulus

modeled by an ideal pulse wave [23]. However, we considered that, for better simulation, ideal shape would be a shape resembling to the real signal shape from the pacemaker cell to the muscle cell in the real heart. Our model based on experiment and the input to the muscle cell has a real shape, measuring the synapse from the pacemaker cell (Fig. 9A). Thus, in our model, the timing and the amplitude of synaptic inputs depend on the membrane potential of the pacemaker cell and the muscle cell, respectively.

In our model, we obtained alternans even though the period of stimulus is unchanged; the pacemaker cell is normal. We chose the several ionic conductances as control parameters. Thus, we could study the mechanism of generating alternans caused by problems such as channelopathies in the muscle cell. We found that free concentration of the potassium ion in the extracellular compartment ($[K]_o$) and the sodium ionic conductance are key parameters to generate alternans. $[K]_o$ affects several other parameters. We studied all of them and found that E_{K1} (the reversal potential for the time-independent potassium current) is the most important parameter correlated with $[K]_o$. Usually the change of E_{K1} only affects the value of the resting membrane potential. However, in this study, we found that the alternating oscillations suddenly appear by a slight increase of E_{K1} .

Extracellular potassium and membrane sodium conductance were key factors for generating alternans (Figs. 9B and 10). An interesting discovery from the present simulation was that alternans was observable only in limited area of simulation plane (Fig. 9B). Too high value of $[K]_o$ suppressed alternans. This is of interest because this finding explains the dying condition of many animals (for example Fig. 5, *Vaspa* and *Ligia*). Edema is one of serious sick state, which accompanies a high heart rate such as the case of a terminal cancer patient. Our simulation can explain this terminal condition. If we observe alternans, we must check whether or not K^+ and/or Na^+ take abnormal values.

It was the first observation of relationship between alternans and the value of both the sodium ionic conductance and the potassium reversal potential. From the biological aspect, an amount of the sodium ion and the potassium ion are controlled by the kidneys. Very sick patients, such as terminal cancer patients, retain a lot of K^+ -leakage from damaged live cells in various organs. This state would worsen the state of the kidneys. Heartbeat checking could be an early warning technology.

Our open problems are as follows: (1) studying the whole network (Fig. 4), (2) investigating calcium dynamics of myocardium. The latter problems are currently under investigation by various researchers (see ref [20]).

APPENDIX

Ionic currents in Eq. (1) are given by

$$I_{Si} = G_{Si} df(V - E_{Si}), \text{ (slow inward current),}$$

$$I_K = G_K XX_i(V - E_K), G_K = 0.282\sqrt{[K]_o/5.4},$$

$$E_K = \frac{RT}{F} \ln \left(\frac{[K]_o + PR_{NaK}[Na]_o}{[K]_i + PR_{NaK}[Na]_i} \right),$$

(time-dependent potassium current),

$$I_{K1} = G_{K1} K_{1\infty}(V - E_{K1}), G_{K1} = 0.6047\sqrt{[K]_o/5.4},$$

$$E_{K1} = \frac{RT}{F} \ln \left(\frac{[K]_o}{[K]_i} \right),$$

(time-dependent potassium current),

$$I_{Kp} = 0.0183Kp(V - E_{Kp}), \text{ (plateau potassium current),}$$

$$I_b = 0.03921(V + 59.87), \text{ (background current).}$$

Detailed explanation of these equations: see Luo-Rudy I model.

REFERENCES

- [1] Goldblatt, C. et al. "Bistability of atmospheric oxygen and the great oxidation." *Nature*. Vol. 443, 2006, pp. 683-686.
- [2] Kawatani, Y., and Hamilton, K., "Weakened stratospheric quasi-biennial oscillation driven by increased tropical mean upwelling." *Nature*, Vol. 497, 2013, pp. 478-481.
- [3] Rosenbaum, D. S. et al. "Electrical alternans and vulnerability to ventricular arrhythmias." *The New England J. of Medicine*, Vol. 330, 1994, pp. 235-241.
- [4] Surawicz, B. et al. "Cardiac alternans: diverse mechanisms and clinical manifestations." *Journal of American College of Cardiology*. Vol. 20, 1992, pp. 483-99.
- [5] Pieske, B. et al. "Alternans goes subcellular. A "disease" of the ryanodine receptor?" *Circulation Research*, Vol. 91, 2002, pp. 553-555.
- [6] Rosenbaum, D.S. et al. "Electrical alternans and vulnerability to ventricular arrhythmias." *N. Engl. J. Med.*, Vol. 330, 1994, pp. 235-241.
- [7] Yazawa, T. et al. "Structure and contractile properties of the ostial muscle (musculus orbicularis ostii) in the heart of the American lobster. *J. Comp. Physiol. B*. Vol. 169, 1999, pp. 529-537.
- [8] Shinozaki, T. et al. "Excitation-contraction coupling in cardiac muscle of lobster (*Homarus americanus*); the role of the sarcolemma and sarcoplasmic reticulum. *J. Comp. Physiol. B*. Vol. 172, 2002, pp. 125-136.
- [9] Wilkens, J. L. et al. "Evolutionary derivation of the American lobster cardiovascular system an hypothesis based on morphological and physiological evidence." *Invertebrate Biol*. Vol. 116, 1997, pp. 30-38.
- [10] Sakurai, A. et al. "Glutamatergic neuromuscular transmission in the heart of the isopod crustacean *Ligia exotica*." *J. Exp. Biol*. Vol. 201, 1998, pp. 2833-2842.
- [11] Yazawa, T. et al. "A pharmacological and HPLC analysis of the excitatory transmitters of the cardiac ganglion in the heart of the isopod crustacean, *Bathynomus doederleini*." *Can. J. Physiol. Pharmacol*. Vol. 76, 1998, pp. 599-604.
- [12] Yazawa, T. et al. "Dopaminergic acceleration and GABAergic inhibition in extrinsic neural control of the hermit crab heart." *J. Comp. Physiol. A*. Vol. 174, 1994, pp. 65-75.
- [13] Yazawa, T. et al. "Intrinsic and extrinsic neural and neurohumoral control of the decapod heart." *Experientia*, Vol. 48, 1992, pp. 834-840.
- [14] Takens, F. "Detecting strange attractors in turbulence." *Lecture Notes in Mathematics*, 1981, pp. 366-381.
- [15] Sakurai, A. et al. "Tension sensitivity of the heart pacemaker neurons in the isopod crustacean *Ligia pallasii*." *J. Exp. Biol.*, Vol. 206, 2003, pp. 105-115.
- [16] Berger, C.M. et al. "Period-doubling bifurcation to alternans in paced cardiac tissue: crossover from smooth to border-collision characteristics." *Phys. Rev. Lett.*, Vol. 99, 2007, 058101.
- [17] Arce, H. et al. "Triggered alternans in an ionic model of ischemic cardiac ventricular muscle." *Chaos*, Vol. 12, 2002, pp. 807-818.
- [18] Bauer, S. et al. "Alternans and the influence of ionic channel modifications: Cardiac three-dimensional simulations and one-dimensional numerical bifurcation analysis." *Chaos*, Vol. 17, 2007, 015104.
- [19] Kitajima, H. et al. "Analysis of a cardiac mathematical model for suppressing alternans." *IEICE Tech. Repo. NLP2010-123*, 2010, pp. 61-64.
- [20] Kitajima, H. et al. "Modified Luo-Rudy model and its bifurcation analysis for suppressing alternans." *Proc. NOLTA*, 2011, pp. 390-393.
- [21] Yanagihara, K. et al. "Reconstruction of sinoatrial node pacemaker potential based on the voltage clamp experiments." *Jpn. J. Physiol.*, Vol. 30, 1980, pp. 841-857.
- [22] Luo, C.H. et al. "A model of the ventricular cardiac action potential. Demoralization, repolarization, and their interaction." *Circ. Res.*, Vol. 68, 1991, pp. 1501-1526.
- [23] Thul, R. et al. "Understanding cardiac alternans: A piecewise linear modeling framework." *Chaos*, Vol. 20, 2010, 045102.